Materials and Structures (2023) 56:90
https://doi.org/10.1617/s11527-023-02173-1

RILEM TC 266-MRP: round-robin rheological tests on high performance mortar and concrete with adapted rheology—rheometers, mixtures and procedures

Dimitri Feys · Mohammed Sonebi · Sofiane Amziane · Chafika Djelal · Khadija El-Cheikh · Shirin Fataei · Markus Greim · Irina Ivanova · Helena Keller · Kamal Khayat · Laurent Libessart · Viktor Mechtcherine · Ivan Navarrete · Arnaud Perrot · Egor Secrieru · Yannick Vanhove

Received: 17 November 2022 / Accepted: 15 April 2023 / Published online: 10 May 2023

Abstract Recent developments in understanding the rheology of mortar and concrete as well as applying this understanding in the practice of construction necessitate an accurate assessment of materials' rheological properties. It is well known that different rheometers for mortar and concrete deliver different results, as this was shown over 15 years ago in two measuring campaigns comparing concrete rheometers. Considering newly developed rheometers, including those to evaluate interface rheology and structural build-up at rest, as well as additional measurement procedures and data interpretation techniques, a new comparison campaign was carried out in 2018 at the Université d'Artois, in Bethune, France. This new campaign focused on measuring workability characteristics, flow curves, static yield stress values, interface properties and tribological data. A total of 14 different devices capable of measuring one or more of the above-mentioned characteristics were employed. These devices included four ICAR rheometers, the Viskomat XL, the eBT-V, the RheoCAD (two geometries), the 4SCC rheometer (two geometries), the plate test, the sliding pipe rheometer, a tribometer and an interface tool for the ICAR rheometer. This paper describes the mixture design and rationale of the five investigated concrete and three investigated mortar mixtures, design and analysis of the experiments, and comparison of test results. The findings confirmed some of the conclusions from two previous testing campaigns and expanded the findings to more modern concrete mixtures and more diversified sets of

This document is the result of an experimental campaign supported by and carried out by a taskgroup of RILEM TC 266-MRP. All members of the taskgroup are listed as authors for this paper, except for Faber Fabbris from EQIOM concrete. The following individuals are the members of RILEM TC 266-MRP who were not involved in the taskgroup: Rolands Cepuritis, Geert De Schutter, Siamak Fakhraei, Steffen Grunewald, Michael Haist, Stefan Jacobsen, Karel Lesage, Julian Link, Dirk Lowke, Tilo Proske, Nicolas Roussel, Wolfram Schmidt, Jon E. Wallevik, Ammar Yahia, and Jiang Zhu. This paper was reviewed and approved by all members of the committee.

D. Feys (✉) · K. Khayat
Department of Civil, Architectural and Environmental Engineering, Missouri University of Science and Technology, Rolla, MO 65409, USA
e-mail: feysd@mst.edu

M. Sonebi
School of Natural and Built Environment, Queen's University Belfast, Belfast BT7 1NN, UK

S. Amziane
Université Clermont Auvergne, CNRS, SIGMA Clermont, Institut Pascal, 63000 Clermont-Ferrand, France

C. Djelal · L. Libessart · Y. Vanhove
University Artois, IMT Lille Douai, Junia, University Lille, ULR 4515, Laboratoire de Génie Civil et géoEnvironnement (LGCgE), 62400 Béthune, France

rheological devices. The investigated rheometers yielded different absolute values for material parameters, but they all were able to similarly distinguish between mixtures qualitatively. For static yield stress and interface rheology measurements, similar conclusions were obtained as for flow curves.

Keywords Rheometer · Concrete · Mortar · Yield stress · Viscosity · Thixotropy · Interface rheometry · Tribology

1 Introduction

The application of rheology in the field of cement-based materials has evolved tremendously in the last 20 years. This has been made possible through a better understanding of the effect of mixture design on rheological properties [1, 2], better measurement tools, a more profound grasp of fluid dynamics concepts applied on concrete materials [3], and the use of numerical simulations [4–7]. However, measuring rheological properties on cement-based materials remains a challenging task [8], and it is known from previous studies that different rheometers may deliver varying rheological values for the same mixtures [9, 10]. Two major rheometer comparison campaigns were held in Nantes (France) in 2000 [9] and in Cleveland (USA) in 2003 [10]. These campaigns showed that, in general, the rheometers could distinguish similar trends in (dynamic) yield stress and plastic viscosity; however, differences were systematically observed in absolute values.

Although not discussed in detail, the authors reported that differences between concrete rheometers can be attributed to two main causes:

- Differences in assessment of torque and rotational velocity values, assuming most rheometers work based on the same principle; and
- Imperfect flow in the rheometer, compared to the ideal conditions required by the transformation equations, which also includes measurement artefacts.

Most rheometers for mortar and concrete are rotational rheometers, and raw data are determined from a component measuring values related to the torque, and a component measuring values related to the angular displacement or rotational velocity. Differences in assessment techniques and methodologies could lead to spreads in registered values, even if the geometry of the rheometer remained unchanged [11]. Knowing the sensitivity and capacity limits of sensors on maximum and minimum values are the key to successful use of a rheometer [12, 13]. Another important factor affecting the results is the calibration of the rheometer and how that is carried out or what it is based on. Are the torque and rotational velocity values uniquely based on the calibrated sensors, or is there a modification factor used in the software or hardware making the data fit the expected properties of a reference fluid? Another factor affecting the results involves the magnitude of the drift of the sensors over time.

The second cause for differences between concrete rheometers is the imperfect flow of the material inside the rheometer container. Most transformation equations to deduct fundamental rheological properties from torque and rotational velocity values assume, inter alia, a homogeneous material, a uniform one-dimensional flow, a perfectly cylindrical geometry, no-slip conditions between the rheometer walls and the material, and no secondary flow [14]. These conditions are not ideally fulfilled when dealing with

K. El-Cheikh
Department of Structural Engineering and Building Materials, Magnel-Vandepitte Laboratory, Technologiepark-Zwijnaarde 60, 9052 Ghent, Belgium

S. Fataei · I. Ivanova · V. Mechtcherine
Institute for Construction Materials, TU Dresden, 01062 Dresden, Germany

M. Greim · H. Keller
Schleibinger Geräte Teubert u. Greim GmbH, 84428 Buchbach, Germany

I. Navarrete
Facultad de Ingeniería y Ciencias, Escuela de Ingeniería Civil en Obras Civiles, Universidad Diego Portales, Av. Ejercito 441, Santiago, Chile

A. Perrot
University of Bretagne-Sud, UMR CNRS 6027, IRDL, 56100 Lorient, France

E. Secrieru
Engineering and Innovation, HeidelbergCement AG, 69181 Leimen, Germany

mortar or concrete. First, the presence of large particles contradicts the homogeneity assumption. The rheometers should have sufficiently large dimensions to reduce the effect of singular particle interactions within the sheared region [15]. Furthermore, particles near a smooth wall surface cause the geometrical wall effect, leading to a non-uniform particle distribution over the volume under consideration. As such, roughness on the rheometer surfaces is needed to reduce the slip and wall effect [16], which is typically implemented by adding ribs or using a vane geometry, which in their turn could cause secondary effects. Shear-induced and gravity-induced particle migration can render the material non-homogeneous during the rheological measurement [17–19]. The presence of ribs or a vane could further cause a deviation from the perfect cylindrical geometry, with the assumption that the circumscribing polygon is sufficiently close to a circle [20, 21]. Lastly, almost every rheometer uses a container, which induces secondary flows at the bottom (and potentially the top) of the flow domain [14, 22].

Due to these concerns, an initiative was launched within RILEM TC 266-MRP, the technical committee dealing with measuring rheological properties of cement-based materials. A subgroup of this committee has agreed to perform a comprehensive round-robin testing campaign to compare concrete rheometers. The 3-day testing program was organized by Drs. Yannick Vanhove and Chafika Djelal at the Universite d'Artois in Bethune, France in May 2018. The campaign assembled collaborators from 10 different companies and research institutes from Belgium, Chile, France, Germany, the United Kingdom, and the United States. While technically this campaign does not fully qualify as a round-robin test, as no material was shipped between laboratories, it is the authors' opinion that bringing all equipment to one location is the only correct way of performing such tests. The rheological properties of cement-based materials are sensitive to constituent materials, mixing energy and environmental conditions. Therefore, all teams assembled in one laboratory with each team using their own devices on the same batch of concrete delivered by the ready-mix company.

The rheological testing campaign did not only focus on measuring flow curves, leading to the determination of (dynamic) yield stress and plastic viscosity but two other parameters were also investigated: the structural build-up and the interface resistance. Recent research has demonstrated the positive and negative effects of structural build-up on the casting process of self-consolidating concrete (SCC) and more recently in 3D-printing of cement-based materials [23–26]. The structural build-up is caused by the flocculation and hydration of cementitious materials and can result in the increase of the static yield stress with rest time. As such, the testing campaign included an assessment of the development of the structural build-up of the investigated mortar and concrete mixtures using devices capable of executing such measurements. Another parameter under investigation was the interface resistance between a smooth wall and concrete, to either identify the friction between the wall and the material under pressure or to predict pressure when concrete is being pumped [27–29].

In total, 14 different devices capable of measuring one or more of the above-mentioned characteristics were employed in the testing program. The test devices are briefly described in this paper and included four ICAR rheometers, the Viskomat XL, the eBT-V, the RheoCAD (two geometries), the 4SCC rheometer (two geometries), the plate test, the sliding pipe rheometer (SLIPER), a tribometer and an interface tool for the ICAR rheometer. The paper at hand also includes a brief description of the rheological testing devices employed during the testing campaign, the designs of the concrete and mortar mixtures, the rationale behind the modifications of the mixture designs, as well as the testing and analysis procedures for the flow curve, structural build-up and interface rheometry measurements. The detailed interpretations of the test results can be found in three upcoming contributions from the team that compare the different devices to evaluate flow curve, structural build-up and interface rheometry data.

2 Rheometers

In total, nine different rheometer types were employed in the testing campaign, including two devices with different geometries for the inner cylinder. However, not all devices were suitable to measure flow curves, structural build-up and interface properties. Table 1 summarizes the technical capabilities of each rheometer to execute a certain measurement and Fig. 1 shows each of the devices. Figure 2 shows a comparison

between the different dimensions of each rheometer capable of measuring flow curves. The sections below provide a brief description of each device. For some rheometers, the flow curve could only be determined in relative units, as the geometry was too complex to allow for an analytical calculation of the fundamental rheological properties. Specific calibrations or numerical simulations could be performed for those devices to obtain fundamental values; however, this was out of the scope of this testing campaign.

2.1 ICAR rheometer

The ICAR rheometer is a portable concrete rheometer, based on the principle of the concentric cylinders system. The inner cylinder is a four-bladed vane, with an inner radius of 63.5 mm and a height of 127 mm. The outer radius, measured up to the tips of the ribs, is 143 mm. This results in a gap between the inner and outer cylinders of 80 mm, which is four times the recommended maximum aggregate size of 20 mm. The distance between the bottom of the vane and the bottom of the bucket is also 80 mm. The concrete volume required is approximately 16 L. The ICAR software allows imposing a constant pre-shear, followed by either an increasing or decreasing flow curve, with a maximum rotational velocity of 0.6 rps. The maximum torque is 25 Nm. The device is also capable of imposing a constant rotational velocity to determine the static yield stress values. The duration of any of the constant shear rate steps can also be programmed. Data registration is at an approximate frequency of 20 Hz. The software automatically calculates flow curve and static yield stress values in fundamental units. For the calculation of dynamic yield stress and plastic viscosity, the software uses a methodology to consider plug flow. However, for the analysis in this testing campaign, the raw data were used to calculate all of the parameters manually. Four ICAR rheometers were used during this campaign.

2.2 Viskomat XL rheometer

The Viskomat XL is a stationary mortar and concrete rheometer capable of determining the rheological properties of concrete with a maximum particle size of 16 mm. The rheometer is based on the principle of concentric cylinders, and the inner cylinder geometry can be selected from a series of probes. A six-bladed vane with a radius of 34.5 mm and a height of 69 mm was used for the measurements. The outer radius is 82.5 mm providing a gap between the inner and outer cylinder of 48 mm. The required concrete volume is approximately 3 L. This rheometer allows for flexible step-like or ramp-like rheometry profiles, including stress-control and oscillatory modes. The load cell has a maximum capacity of 10 Nm, while the rotational velocity can be varied freely between nearly 0 and 1.33 rps.

2.3 eBT-V rheometer

The eBT-V rheometer is a portable device able to measure the rheological properties of mortar and concrete with a maximum particle size of 32 mm. This device can be operated in two different modes: a P-mode (probe-mode), more suitable for conventional vibrated concrete or very stiff concrete, and a V-mode

Table 1 Test types performed by each rheometer

	Flow curve	Thixotropy	Interface properties
ICAR with vane	Yes	Yes	
ICAR with interface tool			Yes
Viskomat XL	Yes	Yes	
eBT-V	Yes	Yes	
RheoCAD with vane	Yes	Yes	
RheoCAD with helix	Yes, but relative units		
4SCC with mixer	Yes, but relative units		
4SCC with Mk-II	yes, but relative units		
Plate test		Yes	
SLIPER			Yes
Plane/plane tribometer			Yes

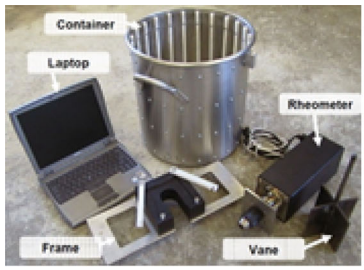

a) ICAR Rheometer

b) Viskomat XL Rheometer

c) eBT-V Rheometer

d) RheoCad Rheometer

e) ConTec 4SCCRheometer

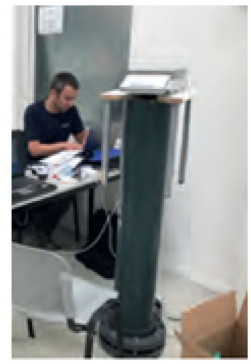

f) Plate Test Method

g) SLIPER Rheometer

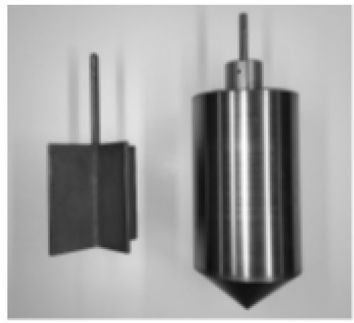

h) Vane (left) and interface tool (right) for ICAR

i) Plane/Plane Tribometer

Fig. 1 Rheometers employed in the round-robin test

(vane-mode) for more flowable mixtures. The measurement profiles can be adjusted according to the measurement mode and the mixture type evaluated. For the measurement campaign, the V-mode was consistently used. The vane has six blades with a radius of 51.5 mm and a height of 103 mm. A concrete volume of 15 L is required. A device holder with rods is inserted in the containing bowl to prevent wall slippage. The outer radius for the V-mode modus is 122 mm providing a gap of 70.5 mm. This mobile rheometer allows to perform rheometric measurements following flexible step-like or ramp-like measurement profiles with a maximum rotational velocity of 0.67 rps and a maximum torque measurement of 10 Nm. The operation of the rheometer and the data acquisition take place by means of a Bluetooth

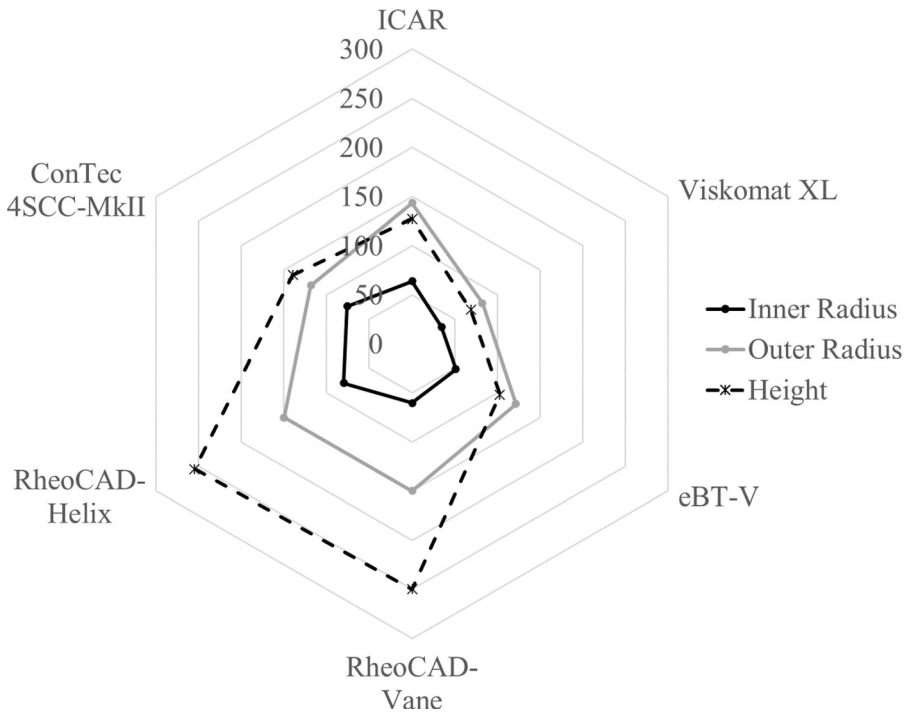

Fig. 2 Comparison of dimensions of rheometers. All units are expressed in mm. The difference between the solid black line (R_i) and the solid gray line (R_o) indicates the gap between the two radii

connection with a smartphone and enables direct display of the measurement results. For the analysis in this testing campaign, the raw data were exported as an excel file for manual calculation of rheological parameters.

2.4 RheoCAD rheometer

The RheoCAD500 rheometer is a stationary concentric cylinder rheometer. The inner cylinder is either a four-bladed vane with a radius of 60 mm and a height of 250 mm, or a helical screw with a radius of 80 mm and a height of 255 mm. The outer cylinder is the concrete bucket with an outer radius of 150 mm and a height of 350 mm. A cage is inserted at the outer edge of the rheometer to avoid slippage. The maximum capacity of the load cell is 10 Nm, and the rheometer has a maximum rotational velocity of 4.1 rps. The required material volume is approximately 30 L. Due to the complex geometry of the helix, no fundamental parameters are calculated for this geometry.

2.5 ConTec 4SCCRheometer

This concrete rheometer is developed as a portable version of the ConTec series, suitable to measure the rheological properties of flowable mixtures with yield stress values up to 120 Pa and plastic viscosity values up to 120 Pa s. The maximum aggregate size allowed is 22 mm and the required concrete volume is 7 L. Two geometries are available to use for the inner cylinder: a mixer-type device and an interrupted helical screw, inspired by the Tattersall Mk-II rheometer. The largest distance between the tips of the blades for the interrupted helical screw was 152 mm in horizontal direction (leading to an "inner radius" of 76 mm) and 140 mm in vertical direction. The radius of the bucket was 118.5 mm. Due to the complex shape of either geometry, no fundamental rheological units for this device were obtained.

2.6 Plate test method

The plate test method was developed as a simple measurement for structural build-up over time. The measurement is based on the determination of the

mass change of a tool submerged in mortar and concrete, which reflects the change in static yield stress with time. A total of 12 measurements per minute are used for this test. The tool is submerged in concrete in a 1.5 m high and 200 mm diameter column, requiring 45 L of mortar or concrete. A ribbed steel rebar with a diameter of 15 mm and a length of 130 mm was selected for the concrete mixtures, while a screw with a diameter of 14 mm and a length of 80 mm was employed for the mortar mixtures. This enabled the adjustment of the roughness of the submerged tool to the particle size of the test sample. This device is only capable of measuring static yield stress variations with time and was only used for the structural build-up measurements.

2.7 SLIPER

The sliding pipe rheometer, or SLIPER, was developed by Kasten as a portable assessment tool for pumping characteristics of concrete [30]. It consists of a plexiglass pipe with 126 mm diameter and 500 mm operational height, which can slide down vertically based on weights added to the system. To operate the SLIPER, 7 L of concrete are required. This device enables a reliable estimation of the flow rate and resulting pumping pressure. While the pipe slides, the concrete is held stationary on top of a pressure sensor. By determining the pressure and velocity at which the pipe slides downwards, a relationship between pumping pressure and flow rate can be determined. The concrete inside the pipe is pre-conditioned by sliding the pipe several times to create the so-called lubrication layer prior to the actual measurement. For the analysis in this testing campaign, the measured pressure and corresponding velocity values were exported and analyzed according to the Bingham model providing rheological parameters for the interface.

2.8 Interface tool for ICAR rheometer

Following the initiatives of Kaplan et al. to develop an interface tool to measure the lubrication layer properties, a smooth aluminum cylinder extension was built for the ICAR rheometer [28, 29]. The cylindrical section is 200 mm high and measures 125 mm in diameter. The bottom is conical in shape to allow easy insertion into the concrete. As the rheometer is the ICAR rheometer, a similar quantity of concrete is required as for the rheometer tests: around 16 L. Similar to the SLIPER, the smooth cylinder allows for the formation of the lubrication layer. Based on the rheological properties of the concrete, the lubrication layer properties can be calculated and Kaplan's equations can be employed to predict pumping pressures [28, 29].

2.9 Plane/plane tribometer

The tribometer measures the friction between concrete and a material representative for formwork [31, 32]. An interchangeable plate can be moved at variable speeds up to 300 mm/s. The concrete sample is placed in two 120 mm-diameter cylindrical sample holders, resulting in a sample volume of around 2 L. The pressure (P) of the concrete against the plate can be varied between 30 and 1000 kPa. A tension sensor (load capacity of 17 kN) measures the frictional stress executed during the sliding of the plate. For this campaign, the frictional stress and the coefficient of friction between the mixtures and a steel plate obtained in a formwork face with a roughness value R_a of 1.07 µm were measured. The motor coupled to a worm allows the sliding of the metal plate against the fresh concrete. The displacement rate was 0.84 mm/s, corresponding to a formwork filling rate of 3 m/h. The applied pressure on the concrete varied between 50 and 150 kPa, simulating a concrete height of 2–6 m.

2.10 Workability test methods

During the execution of the flow curve tests (see further for timeline), several fresh concrete tests were carried out. This included the slump or slump flow, T50, V-funnel flow time, L-box and J-Ring passing ability values, as well as density, air content, and temperature.

3 Mixture designs

Tables 2 and 3 display the selected mixture designs for five evaluated concrete and three mortar mixtures, respectively, that were employed in this testing campaign. It was decided to evaluate a number of mortar mixtures for a couple of reasons. Reducing the aggregate size, while maintaining the same gap size,

Table 2 Concrete mix designs (all units are in kg/m^3)

	Concrete 1	Concrete 2	Concrete 3	Concrete 4	Concrete 5
CEM III/A 42.5N	330	330	385	385	385
Limestone filler	170	170	65	25	25
Water	195	195	145	170	170
Coarse aggregate 10/20			650		
Coarse aggregate 6/12	755	755	280	930	930
Crushed sand 0/4	430	430	245	265	265
Natural sand 0/4	430	430	600	615	615
PCP—HRWRA 1	3.3	3.79			
PCP—HRWRA 2			4.62	2.69	2.69
Set retarder				0.39	0.39
VMA					0.77

Table 3 Mortar mix designs (all units are in kg/m^3)

	Mortar 1	Mortar 2	Mortar 3
CEM I 52.5 N	280	280	280
Limestone filler	370	370	370
Water	240	240	240
Crushed sand 0/4	383	383	383
Natural sand 0/4	899	899	899
PCP—HRWRA 1	4.2	4.2	3.78
Set retarder	0.64	0.64	0.64
VMA		0.84	1.68
Shrinkage-reducer	6.5	6.5	6.5
Air-entrainer	0.56	0.56	0.56
Microfibers	0.3	0.3	0.3

can decrease the fluctuation in torque data, which can lead to more stable rheological measurements. Vertical segregation risk can increase proportionally to the maximum particle size, all other parameters remaining constant, and shear-induced particle migration increases with the particle size squared. Selecting mortars as part of the evaluation allows the comparison of the devices while minimizing certain risks affecting or invalidating the measurements.

Concretes 1, 2 and 3 were designed as SCC mixtures. The target slump flows for concretes 1 and 3 were between 550 and 650 mm, while 650–750 mm slump flow was desired for concrete mixture 2. As can be seen in Table 2, the mixture proportioning for concrete mixtures 1 and 2 are identical, apart from the increase in high range water reducer admixture (HRWRA) for mixture 2. As such, a mixture with similar viscosity values, but lower dynamic yield stress was anticipated. Concrete 3 contained considerably less water, and a part of the limestone filler was replaced by cement, creating a more viscous mixture. Concrete mixtures 4 and 5 are based on mixtures suitable for foundation construction, with a decrease in paste volume and an increase in coarse aggregate content compared to the previous concrete mixtures. The 5th concrete mixture had greater rheological properties in terms of yield stress and viscosity values by adding a viscosity-modifying agent (VMA) that is used to enhance stability. No conventional vibrated concrete mixtures were investigated, given issues related to plug flow. If the plug zone in a concentric rheometer is too large, it could lead to an invalid measurement of a flow curve.

The mortar mixtures, which were evaluated on the second day of the campaign, were based on a typical mortar used to create low-thickness flooring. The mortars incorporated a shrinkage-reducing admixture and a low volume of microfibers to reduce the risk of cracking. The imposed changes from mortar 1 to the other two mortars were to create a mixture with a higher viscosity achieved in mortar 2, or a higher yield stress for mortar 3.

The concrete mixtures were prepared with a blended Portland-slag cement (CEM III/A) and limestone powder as a mineral filler. All concrete mixtures contained a combination of crushed and natural sands and a crushed coarse aggregate with a nominal maximum aggregate size (NMS) of 12 mm, except for concrete 3 that had a NMS of 20 mm. Combinations of HRWRA, set retarder and VMA were

employed to achieve the targeted rheological properties. The mortar mixtures were made with similar materials, except that the binder was replaced by an ordinary Portland cement (CEM I) without any slag or filler. An air-entraining admixture, a shrinkage-reducing admixture and microfibers were employed, given the intended application of the delivered mixture design. The mortar mixtures had a NMS of 4 mm.

All mixtures were provided by a commercial ready-mix plant (RMX Production unit of Béthune). Once the mixer arrived at the laboratory, the slump/slump flow, T-50 (if applicable), and visual stability of the mixtures were verified, and adjustments through chemical admixtures were performed, if necessary.

4 Testing sequence

For each concrete and mortar mixture, a fixed testing sequence was followed. After arrival of the mixture to the laboratory, and any adjustments with admixtures if necessary, several wheelbarrows of concrete were sampled for testing. The full testing sequence, including flow curve, structural build-up and interface rheometry tests was as follows:

- 0 min: Initial flow curve test. The start of the initial flow curve test is taken as the reference time for each mixture.
- 10 min: Static yield stress measurement 1, served for determining the thixotropic properties.
- 20 min: Interface rheometry test.
- 40 min: Static yield stress measurement 2, after a 30 min rest time on the same, unaltered sample as static yield stress measurement 1.
- 50 min: Second flow curve test.
- 60 min: Second interface rheometry test.
- 80 min: Third flow curve test.

Table 4 shows the rheometers used for various tests at different times. Fresh concrete tests were executed in parallel with each flow curve test. In between successive tests, the concrete was removed from the rheometer, and the device was cleaned, and a new sample was inserted before the next measurement. In between two static yield stress tests, the concrete was kept inside each rheometer employed for thixotropy evaluation.

Table 4 Testing sequence for each rheometer

	0 min	10 min	20 min	40 min	50 min	60 min	80 min
ICAR 1—Vane	FC	YS		YS	FC		FC
ICAR 2—Vane	FC				FC		FC
ICAR 2—Cylinder			IF			IF	
ICAR 3—Vane	FC				FC		FC
ICAR 4—Vane	FC	YS		YS	FC		FC
eBT-V	FC	YS		YS	FC		FC
Viskomat XL	FC	YS		YS	FC		FC
SLIPER			IF			IF	
RheoCAD—Vane	FC	YS		YS			FC
RheoCAD—Helix					FC		
4SCC—Mixer	FC						FC
4SCC—Mod. MK-II					FC		
Tribometer			IF				
Plate test		Continuous measurement					

FC flow curve; *YS* static yield stress; *IF* interface properties

5 Flow curve testing and analysis procedure

5.1 Testing procedure

It is commonly accepted that Bingham law (Eq. 1) applies to mortar and concrete, with some more exceptional cases showing shear-thinning or shear-thickening. The Bingham law identifies a yield stress (τ_0) and plastic viscosity (μ_p). The yield stress is the stress which needs to be exceeded to ensure flow, while the viscosity is the resistance to an increase in flow rate.

$$\tau = \tau_0 + \mu_p \dot{\gamma} \tag{1}$$

With τ = shear stress (Pa), τ_0 = yield stress (Pa), μ_p = plastic viscosity (Pa s), $\dot{\gamma}$ = shear rate (s^{-1}).

Some best practices for concrete rheology were considered to determine the flow curves. First, the flow curve should be determined when the concrete material is in the reference state corresponding to the highest shear rate applied [33]. As such, a sufficiently long pre-shearing time at the highest rotational velocity is required [8]. This also means that each rheometer should subject the material to approximately the same shear rate, which will be discussed further in this section. Second, the extrapolation towards zero rotational velocity should be kept sufficiently small, but plug flow needs to be considered. Third, the measurement time should be kept sufficiently short to minimize the negative effect of gravity-induced and shear-induced particle migration. Therefore, the adopted flow curve procedure started with a 20 s pre-shear period at maximum rotational velocity. This was followed by a stepwise decreasing curve, containing eight steps of 5 s duration each. It is worth to note that in one case (ICAR 4), the pre-shear period was extended to 60 s and the duration of any shear rate step was set to 15 s, rather than 5 s (as by default setting of the machine).

For the 4SCC rheometer, this procedure was reduced to six steps due to limitations of the software. For the mortar mixtures, the pre-shear period was extended to 30 s. It should also be noted that an empty measurement with the same procedure was performed before each flow curve, to correct for any residual torque in the system or an offset was carried out automatically.

As was mentioned before, in each rheometer, the material should undergo the same shear rate profile. However, this is hard to achieve as the spatial distribution of shear rate in the gap depends strongly on the inner and outer radius of the rheometer [14]. An attempt was made to ensure a constant average shear rate in each rheometer by means of a theoretical calculation. A virtual concrete mixture with fixed rheological properties (τ_0 = 50 Pa, μ_p = 20 Pa s) was assumed for this calculation. Based on the Reiner–Riwlin equation, one can calculate G and H parameters, the intercept of the line with the T-axis and the slope of the line in a T-N diagram, respectively:

$$G_x = \frac{4\pi h_x \ln\left(\frac{R_{o,x}}{R_{i,x}}\right)}{\left(\frac{1}{R_{i,x}^2} - \frac{1}{R_{o,x}^2}\right)} \tau_0 \tag{2}$$

$$H_x = \frac{8\pi^2 h_x}{\left(\frac{1}{R_{i,x}^2} - \frac{1}{R_{o,x}^2}\right)} \mu_p \tag{3}$$

With R_i = inner radius (m), R_o = outer radius (m), h = height (m), G = intercept with T-axis (Nm), H = slope in T-N diagram (Nm s), index x denotes rheometer x

Starting from the most limiting rheometer in terms of rotational velocity, a maximum rotational velocity of 0.5 rps was imposed for the ICAR rheometer. Based on the ICAR's geometry, G and H can be calculated with the chosen rheological properties, and the expected torque value at 0.5 rps can be evaluated as $T_{max,ICAR} = G + 0.5\,H$. Inverting the equation above transforms yield stress into G; replacing G by $T_{max,ICAR}$, one can obtain the expected maximum stress τ_{max} in the rheometer. The resulting magnitude is an average stress value over the gap, and cannot be associated to a certain location in the rheometer. Based on τ_{max} and the known rheological properties, the maximum shear rate in the ICAR rheometer for the assumed virtual concrete can be calculated.

For the Viskomat XL, eBT-V and RheoCAD-vane rheometers, the previous procedure was followed in the opposite direction. From the shear rate, and thus the shear stress determined above, one can calculate $T_{max,x}$ for each rheometer separately. With the altered G and H values—dependent on the geometry—the $N_{max,x}$ value for each rheometer can be calculated

which would lead to the same shear rate as in any other rheometer.

This procedure was performed to determine the maximum rotational velocity for each rheometer. The minimum rotational velocity in the ICAR rheometer was specified to be 0.025 rps, to reduce the size of extrapolation to determine the yield stress. The minimum rotational velocity for the other rheometers was determined by taking the same ratio as for the maximum rotational velocities. The potential for plug flow was not considered in this analysis. Table 5 shows the N_{max} and N_{min} for each rheometer.

For the RheoCAD with the helix tool, the same profile as for the vane tool was imposed, as no analytical equations are available. For the 4SCC rheometer, for the same reasons, the maximum rotational and minimum rotational velocities were set at 0.21 and 0.01 rps, respectively. These values are arbitrary, as no calculation of fundamental properties was available.

As indicated before, for one of the ICAR rheometers (ICAR 4), a different procedure was imposed, consisting of a pre-shear period of 60 s, and six steps decreasing the rotational velocity from 0.6 to 0.1 rps, with steps of 15 s each. However, this relatively long procedure can increase the risk of shear-induced particle migration and segregation. The value of 15 s has been set based on measurement experience, as a practical compromise between a closer appreciation of steady-state properties and short measurement (in order to prevent segregation).

5.2 Analysis procedure

The analysis of the flow curves starts with the interpretation or verification of the zero measurement, which was performed before each flow curve. For each step in the curve, the registered values corresponding to the last 4 s were averaged if no large fluctuations were recorded. Based on those averages, an empty T-N plot was established. If an automatic offset was performed by the rheometer, no empty measurement was needed.

Table 5 N_{max} and N_{min} for each rheometer (in rotations per second)

	N_{max}	N_{min}
ICAR 1-3	0.500	0.025
Viskomat XL	0.540	0.027
eBT-V	0.529	0.026
Rheocad	0.570	0.028
4SCC Rheometer	0.210	0.010

For the flow curves measured on mortar and concrete, the torque was plotted versus time, and for each step, it was verified whether no extreme fluctuations in signal occurred, and the trend of the torque versus time was evaluated: constant, increasing or decreasing. An increasing trend indicates rapid rebuilding of internal structure, and decreasing trend signifies a breakdown of internal structure, meaning the reference state has not yet been reached [8]. It could also be indicative of some kind of particle migration, but this is much more difficult to establish. Points that showed extreme fluctuations or decreasing trends were eliminated from the data set. For the remaining points, the average value of the last 4 s for each step was calculated, leading to eight different T-N points, with an additional point determined at the end of the pre-shear period. It is worth mentioning that there is minimal variation between the average rotational velocities during preceding the empty measurement and during the corresponding concrete or mortar measurement. Accordingly, for each rotational velocity the torque was corrected by subtracting the zero-torque measurement at each corresponding rotational velocity, if non-zero torque values were observed.

From the corrected torque-rotational (T-N) velocity data, the G and H values were extracted, which correspond to the intercept and slope of the torque-rotational velocity relationship, respectively. Initial values of yield stress and plastic viscosity were calculated by inverting Eqs. 2 and 3. This procedure is the standard Reiner–Riwlin procedure for Bingham materials. Based on the evaluation of the T-N curves, a large majority of the measured mixtures can be approximated by the Bingham law. Following the determination of initial rheological parameters, the shear stress at the outer radius of the rheometer, at the lowest average torque value was calculated as follows:

$$\tau_{R_o} = \frac{T_{min-corr}}{2\pi R_o^2 h} \quad (4)$$

where τ_{Ro} = stress at outer radius (Pa), $T_{\text{min-corr}}$ = average torque value at lowest rotational velocity, corrected for the zero measurement (Nm).

The stress at the outer radius was compared to the initial value of the dynamic yield stress. If τ_{Ro} was higher than the dynamic yield stress, the entire flow domain was sheared for the full duration of the measurement, and the obtained rheological properties were final. In the other case, there is an indication that at least a part of the measurement is in plug flow, and the rheological properties need to be corrected. This can be done through an iterative procedure:

- For each rotational velocity, the stress at the inner cylinder is calculated. This stress remains unchanged during the entire calculation procedure:

$$\tau = \frac{T}{2\pi R_{\text{i}}^2 h} \tag{5}$$

- For each rotational velocity, the plug radius (R_{p}) is re-calculated based on the previous (or initial) dynamic yield stress value. This value is variable with each iteration.

$$R_{\text{p}} = \sqrt{\frac{T}{2\pi\tau_{\text{o}} h}} \tag{6}$$

- Each R_{p} value is compared to R_{o} and the smaller of the two is retained as the outer boundary of the flow domain, denoted as R_s.
- The shear rate at the inner cylinder can be calculated by combining the Bingham parameters from the previous iteration and modifying the Reiner–Riwlin equation [5]:

$$\dot{\gamma}_{R_{\text{i}}} = \frac{2}{R_{\text{i}}^2}\left(\frac{1}{R_{\text{i}}^2} - \frac{1}{R_s^2}\right)^{-1}\left(2\pi N + \frac{\tau_0}{\mu_{\text{p}}}\ln\left(\frac{R_s}{R_{\text{i}}}\right)\right) - \frac{\tau_0}{\mu_{\text{p}}} \tag{7}$$

- At each iteration, a series of shear stress—shear rate couples are available, allowing for the calculation of new values of dynamic yield stress and plastic viscosity. These new values are used in the next iteration to calculate plug radius and shear rate values at each rotational velocity.
- The iteration stops when both dynamic yield stress and plastic viscosity do no longer significantly change between each iteration. These are the corrected rheological properties.

As a final step in the analysis procedure, the thickness of the flow domain is calculated. It can be easily derived from the final R_s values in the iterative process above. If $R_s - R_{\text{i}}$ becomes too small, the homogeneity of the material can be questioned. As a criterion for this campaign, the measurement was deemed invalid if $R_s - R_{\text{i}}$ became smaller than $d_{\max}$. If the measurement is invalid, it is not included in the measurements database.

6 Thixotropy testing and analysis

The testing procedure for structural build-up consisted of executing two static yield stress measurements with a 30 min waiting interval in between. Before the first static yield stress measurement, an empty measurement was performed to eliminate any residual torque from the sensor. The average of this measurement, which delivered, approximately, a constant torque value, was subtracted from the final torque readings. As the concrete or mortar was kept inside the container in between two measurements, no zero measurement was performed prior to the second static yield stress determination.

A low rotational velocity was imposed on all rheometers to determine the static yield stress, and the torque was registered. Excessive peaks were eliminated from the measurement if necessary. The maximum torque value was registered if the overall curve showed a peak value. If not, the average of the measured constant torque was calculated. These measurements were corrected for the zero measurement. To calculate static yield stress, the maximum torque was divided by $2\pi {R_{\text{i}}}^2 h$ to obtain the static yield stress.

Concerning the static yield stress, the flow history of the materials is crucial for the estimation of structural build-up indexes of cementitious materials. It is important to stress that each measurement of static yield stress must be coupled to a corresponding resting time.

For the plate test, the early surface settlement of the material must be sufficient to make the sample reach its critical strain and induce shearing at the interface. If the last condition is fulfilled, the friction stress at the

interface between the tool and the test material can be equal to the static yield stress of the material. By writing the force balance equation on the immersed tool, it is possible to compute the evolution of the static yield stress $\tau_{0,s}$ with time at rest [34]:

$$\tau_{0,s}(t) = \frac{g\left(\Delta m_{\text{plate}}(t) + \rho_{\text{concrete}} V_{\text{plate}}\right)}{S_{\text{plate}}} \quad (8)$$

where Δm_{plate} is the mass variation of the plate, ρ_{concrete} is the concrete density, V_{plate} and S_{plate} are the volume and the surface of the immersed part of the plate respectively.

The mass variation of the sample or of the tool is recorded i.e. the apparent mass of the immersed tool or the apparent mass of the sample is continuously monitored versus time by recording the balance output with a computer. This test is close to the moving plate test developed in NIST [35]. The computation of the initial static yield stress is not easy because of the initial state of the concrete (and the moment when sufficient settlement is achieved at the interface). However, it is important to note here that only the variation of static yield stress was computed using this device because of uncertainty on the initial value. In this case, the structural build-up was computed using the following equation [36]:

$$A_{\text{thix}} = \frac{g\Delta(\Delta m_{\text{plate}}(t))}{S_{\text{plate}}\Delta t_{\text{rest}}} \quad (9)$$

7 Interface rheometry testing and analysis

For the interface rheometry test, no uniform procedure was imposed as each device had its specific testing protocol.

Different numbers of slide cycles at different sliding speeds were carried out with the SLIPER. These were 7–10 slides for concrete and 8–16 slides for mortar. The invalid slides were excluded. The direct outputs from SLIPER are pressure (P) and flow rate (Q) results which can be represented in a P-Q diagram. The linear regression of the P-Q diagram provides the intercept point and the slope of P-Q curve. This is accomplished with the yield stress parameter a [mbar] and viscosity parameter b [mbar h/m], which are independent from the geometry of the SLIPER [30] and thus can be used for the calculation of the pumping pressure and flow rate for various pipe lengths. The pressure prediction was done for a pipe length of 100 m and a pipe diameter of 0.125 m.

The interface measurements in the ICAR rheometer with smooth cylinder followed a testing procedure identical to the flow curves: a pre-shear period of 20 s at 0.5 rps was imposed to create the lubrication layer, followed by a stepwise decrease in rotational velocity from 0.5 to 0.025 rps, in eight steps of 5 s each. Torque data were averaged for each step if equilibrium was observed, and the torque values were corrected with a zero measurement. The reported values are the slope of the T-N line based on the raw data. One can also calculate the lubrication layer properties (yield stress and viscous constant) according to the procedure described in [29]. This aspect will be discussed in another contribution from this team.

For the tribometer, the displacement of the plate at the concrete/plate interface created a tangential friction force that is opposed to the force of displacement. For each test, the tangential (or frictional) force F_{mes} that resists the transverse movement of the plate was measured with a load cell and is the sum of two friction components: a friction force generated by the sealing system of the sample holders (F_v) and a friction force induced by the fresh concrete in contact with each of the two faces of the plate ($2.F_b$) considering the symmetry of the system. F_v is measured by displacing the plane plate without concrete prior to each test.

$$F_{\text{mes}} = F_v + 2.F_b \quad (10)$$

The frictional stress τ_b of the concrete is calculated by dividing the friction force F_b with the concrete surface S_c according to:

$$\tau = \frac{F_b}{S_c} = \frac{2(F_{\text{mes}} - F_v)}{\pi d^2} \quad (11)$$

where d is the sample-holder diameter of 120 mm.

The coefficient of friction value (μ) describes the ratio of the concrete friction stress and the contact pressure P of the concrete against the metallic plate.

$$\tau = \mu \cdot P \quad (12)$$

8 Results

Table 6 shows the fresh concrete results, executed simultaneously with all flow curves.

Figures 3 and 4 show the results of the obtained yield stress and plastic viscosity values for all valid flow curve tests. It should be noted though that all results from the ICAR rheometers, eBT-V, Viskomat XL and RheoCAD—Vane were determined according to the procedure described in Sect. 5, and the results are calculated in Pa and Pa s, and plotted on the left axes in Figs. 3 and 4. For the RheoCAD—Helix, there are no transformation equations available. As such, the intercept G and slope H of the torque-rotational velocity curve were extracted, and plotted on the right axes in Figs. 3 and 4. Similarly for the 4SCC Rheometer, results were in relative units (in A for *G* and A s for *H*), also plotted on the right side of Figs. 3 and 4.

At first sight, the data in Figs. 3 and 4 show a relatively large scatter, but some of that scatter, especially for concrete viscosity, can be attributed to the results from the RheoCAD—Helix and the 4SCC with the mixer tool. While focusing on the other employed devices in the graphs shows that most rheometers are able to distinguish between different levels of yield stress and viscosity, but that there are differences between the devices. The larger the absolute value of yield stress or viscosity, the larger the scatter appears to be. In general, these results are in line with the results obtained two decades ago in the two testing campaigns on concrete rheometers [9, 10].

Figure 5 shows the static yield stress values obtained according to the procedure described in Sect. 6, for all valid tests. Similar to Figs. 3 and 4, Fig. 5 shows that, in most cases, the rheometers are able to distinguish between different levels of static yield stress, and a higher static yield stress value seems to generate more scatter in the data.

Table 6 Fresh concrete test results

Mixture—elapsed time	SF/slump	T500	VF	L-box	JR	Air	Dens	FT
C1—0 min	600	2.3	22	0.33	545	1.8	2455	
C1—50 min	480	7.2	47					
C1—80 min	425	–	39					
C2—0 min	705	1.2	5	0.81	655	1.2	2470	
C2—50 min	655	1.6	18					
C2—80 min	595	2.8	11					
C3—0 min	545	5.7	–	0.51	505	1.7	2514	640
C3—50 min	555	5.7	22					325
C3—80 min	490	14.0	53					600
C4—0 min	610	2.1	19	0.24	600	1.5	2459	
C4—50 min	595	2.9	9					
C4—80 min	540	4.5	12					
C5—0 min	405 / 230	–	–	0.21	–	2.0	2434	575
C5—50 min	430 / 240	–	–					
C5—80 min	410	–	–					
M1—0 min	735	1.4	3.1			3.5	2235	
M1—50 min	735	2.1	4.0					
M1—80 min	710	2.2	3.8					
M2—0 min	660	2.2	4.4			3.5	2220	
M2—50 min	640	2.3	5.1					
M2—80 min	635	2.7	3.6					
M3—0 min	565	1.6	3.3			4.0	2170	
M3—50 min	615	1.6	4.0					
M3—80 min	560	2.0	4.4					

SF slump flow (in mm), T50 (in s), *VF* V-funnel flow time (in s), L-box filling ratio (–), *JR* J-Ring final diameter (in mm), air content (%), density (in kg/m^3) and the DIN *FT* flow table (in mm)

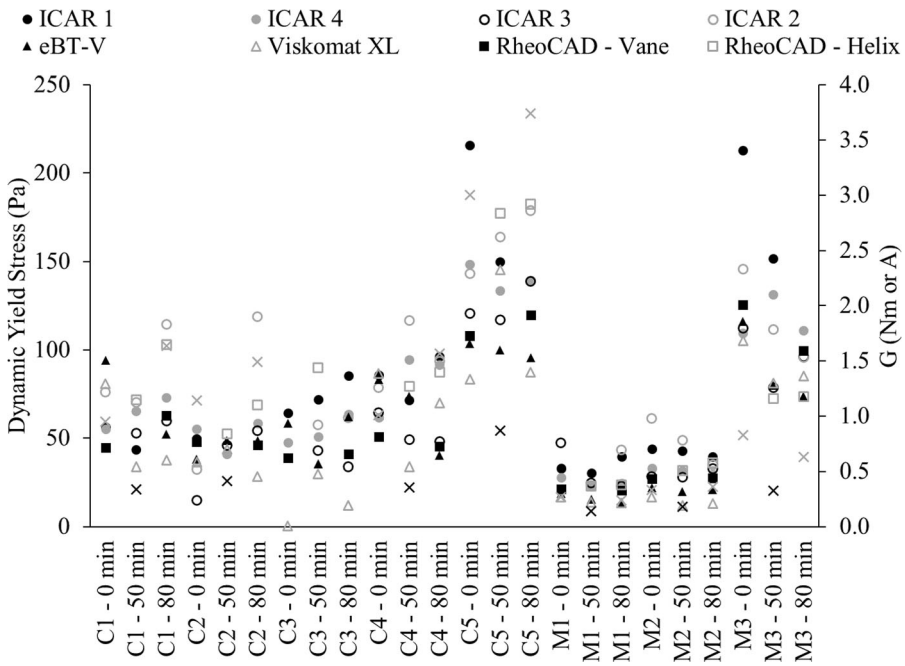

Fig. 3 Dynamic yield stress or *G* for all rheometers and for all valid flow curve tests performed

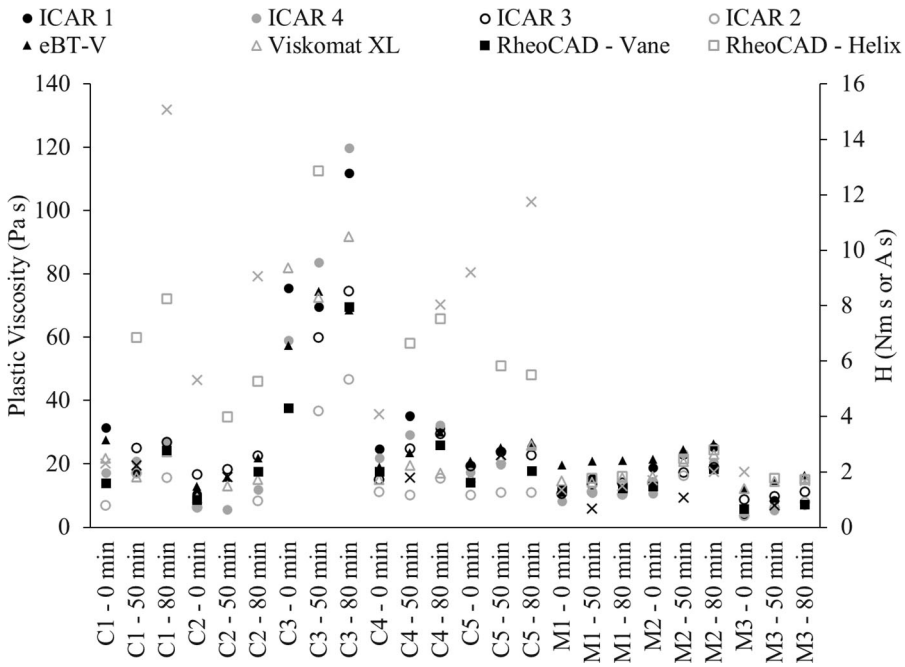

Fig. 4 Plastic viscosity or *H* for all rheometers and all valid flow curve tests performed

Figure 6 shows the results of the SLIPER and ICAR interface rheometer, following the procedures in Sect. 7. For the SLIPER, the obtained intercept "*a*", in mbar, and slope "*b*" in mbar h/m are derived from the data. For the ICAR with interface device, intercept, in Nm, and slope, in Nm s, are determined from the T-N graph. From Fig. 6, it can be seen that the slope values, representing an increase in flow resistance with

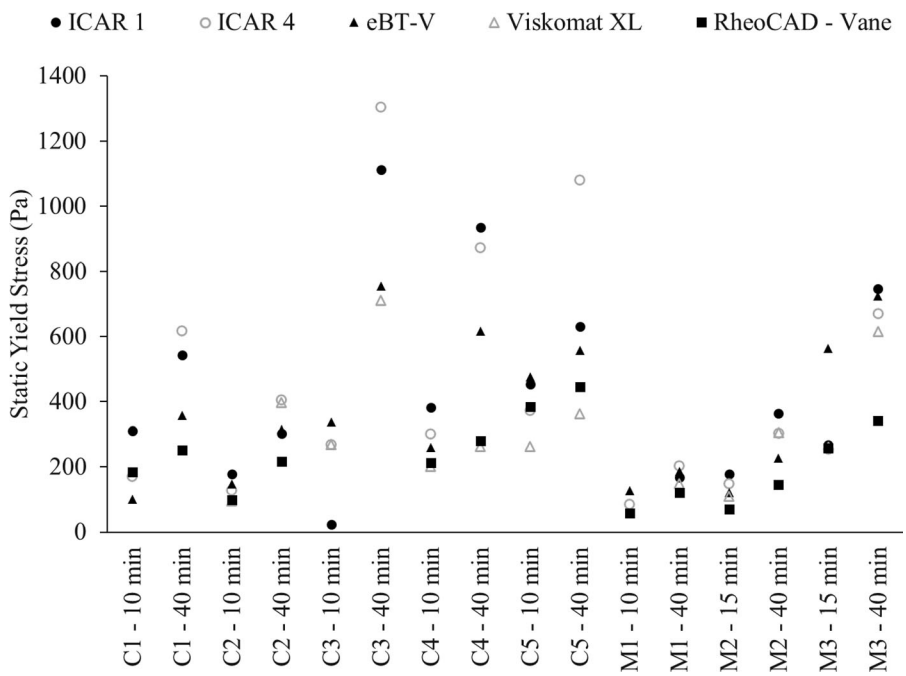

Fig. 5 Static yield stress values obtained with the different rheometers, for all valid static yield stress tests

an increase in flow rate during pumping, distinguish between mixtures in similar ways, although some deviations can be observed. These could, however, be attributed to the large differences in intercept values between both devices.

The stress values related to different contact pressures at 10 and 20 min are shown in Fig. 7. Linear regression is obtained for each concrete mixture based on Coulomb's law (Eq. 12) with a high correlation coefficient (R^2) of 0.88–0.95. As shown in Figure 7, tests realized on a short time at 10 and 20 min do not change the slope values which represent the coefficient of friction determined from Eq. 12. The maximum friction coefficient of 0.19 was obtained for the mixture C5 which has the lowest concrete slump flow value of 405 m. Conversely, the C2 mixture has the lowest coefficient of friction for a concrete slump value of 705 mm. These results show that the concrete workability can be related to the friction.

For any of the data sets on flow curves, thixotropy and interface rheometry tests, the research team has prepared additional contributions with more in-depth comparisons and analyses on the sensitivity and performance of the various testing devices.

9 Conclusions

After a hiatus of 15 years, a concrete rheometer comparison campaign was carried out at the Universite d'Artois, in Bethune, France in May of 2018. It consisted of evaluating the performance of 14 testing devices: 4 ICAR rheometers, the eBT-V, the Viskomat XL, the RheoCAD with vane and helix geometry, the 4SCC rheometer with Mk-II cylinder and mixer, the plate test, the SLIPER, an interface rheometry cylinder mounted on an ICAR rheometer and a plane/plane tribometer for friction. The comparison was performed with five concrete and three mortar mixtures. All compositions were sufficiently flowable to enhance the validity of the obtained data. The mixture designs were varied to obtain significant differences in rheological properties between the mixtures corresponding to modern concretes.

In contrast to previous campaigns, this comparison has included measurements other than flow curves. Thixotropy and interface rheology were also determined with different suitable devices. For each measurement type: flow curves, thixotropy and interface rheometry, a special testing and analysis procedure was developed to facilitate comparing devices

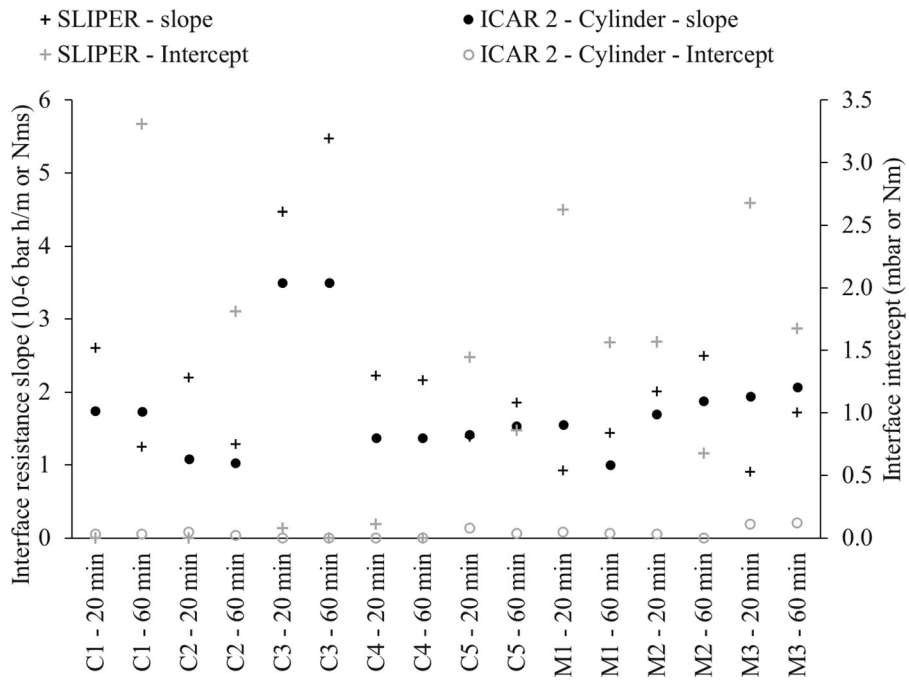

Fig. 6 Interface rheometry data for SLIPER (+ symbols) and ICAR rheometer with interface tool (circular symbols). The results are divided into slope (black—left axis) and intercept (gray—right axis)

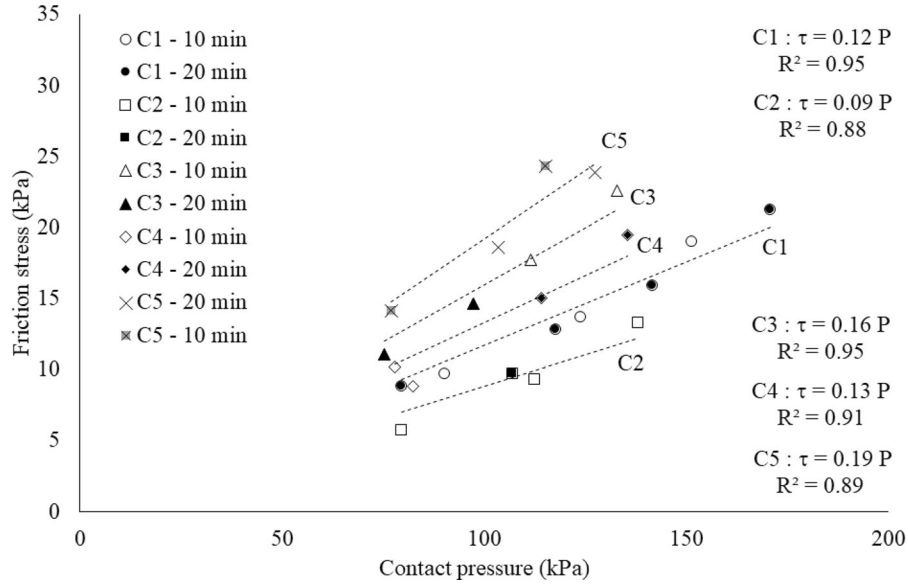

Fig. 7 Friction stress and friction coefficient values at 10 and 20 min (v = 0.84 mm/s)

and to eliminate any potential errors in assessment and interpretation of the data.

With the new devices developed in the last 15 years, the results strengthen the main outcomes obtained in previous campaigns: most rheometers are found to be able to determine the distinct levels of rheological properties, but differences between absolute values remain observable. This observation was

found for the flow curves, static yield stress and interface rheometry measurements. The sources for the differences in values are assumed to stem from errors in calibration and data assessment, which should induce a difference between the devices independent of the mixtures, and the imperfect flow behavior inside the rheometer, providing inaccuracies in the transformation into fundamental units. This latter source of difference should to some extent be dependent on the mixture composition and properties. More details on analysis and interpretation of flow curves, structural build-up and interface rheometry can be found, separately, in different contributions from the research team.

Acknowledgements The authors would like to acknowledge EQIOM Concrete for the donation, delivery and adjustment of the investigated mixtures. The technical support of the mix design team of EQIOM Concrete in changing the rheological properties of the mixtures to suit the testing program is greatly appreciated. The authors wish to express their gratitude and sincere appreciation to the French Group of Rheology (GFR), the agglomeration community Artois Com, the French National Federation of Public Works (FNTP), the Structure&Réhabilitation company, The Université d'Artois and the Laboratoire de Génie Civil et géo-Environnement (LGCgE) for giving financial support to perform this study. The authors acknowledge the support of the Civil Engineering Department of the Université d'Artois for making their facilities available to the research team, as well as Francis Thibaut (technical staff), Sacha Crepelle, Apolline Dilly, Agnaou Elhachemi, Salim Hammoumi, Issam Laiymani and Edouard Morel (students) for their help during three intensive days of testing.

Declarations

Conflict of interest None of the authors declare a conflict of interest.

References

1. Tattersall G, Banfill P (1983) The rheology of fresh concrete. Pitman, London
2. Ovarlez G (2012) Introduction of the rheometry of complex suspensions. In: Roussel N (ed) Understanding the rheology of concrete. Woodhead Publishing Limited, Cambridge, pp 23–62
3. Mechtcherine V, Gram A, Krenzer K, Schwabe J-H, Shyshko S, Roussel N (2014) Simulation of fresh concrete flow using discrete element method (DEM): theory and applications. Mater Struct 47:615–630
4. Roussel N, Geiker M, Dufour F, Thrane L, Szabo P (2007) Computational modeling of concrete flow: general overview. Cem Concr Res 37(9):1298–1307
5. Wallevik J (2003) Rheology of particle suspensions: fresh concrete, mortar and cement paste with various types of lignosulfonates. PhD dissertation, The Norwegian University of Science and Technology (NTNU)
6. Vasilic K, Gram A, Wallevik JE (2019) Numerical simulation of fresh concrete flow: insight and challenges. RILEM Tech Lett 4:57–66
7. Wallevik JE, Wallevik OH (2017) Analysis of shear rate inside a concrete truck mixer. Cem Concr Res 95:9–17
8. Wallevik O, Feys D, Wallevik J, Khayat K (2015) Avoiding inaccurate interpretations of rheological measurements for cement-based materials. Cem Concr Res 78:100–109
9. Banfill P, Beaupré D, Chapdelaine F, de Larrard F, Domone P, Nachbaur L, Sedran T, Wallevik O, Wallevik JE (2000) Comparison of concrete rheometers: international tests at LCPC, Nantes. NISTIR 6819
10. Ferraris CF, Brower LE, Beaupré D, Chapdelaine F, Struble L, Domone P, Koehler E, Lin S, Sonebi M, Struble L, Tepke D, Wallevik O, Wallevik JE (2003) Comparison of concrete rheometers: international tests at MB, Cleveland OH, USA. NISTIR 7154
11. Haist M, Link J, Nicia D, Leinitz S, Baumert C, von Bronk T, Cotardo D, Eslami Pirharati M, Fataei S, Garrecht H, Gehlen C, Hauschildt I, Ivanova I, Jesinghausen S, Klein C, Krauss H-W, Lohaus L, Lowke D, Mazanec O, Pawelczyk S, Pott U, Radebe NW, Riedmiller JJ, Schmid H-J, Schmidt W, Secrieru E, Stephan D, Thiedeitz M, Wilhelm M, Mechtcherine V (2020) Interlaboratory study on rheological properties of cement pastes and reference substances: comparability of measurements performed with different rheometers and measurement geometries. Mater Struct 53:92
12. Ferraris CF, Martys NS (2012) Concrete rheometers. In: Roussel N (ed) Understanding rheology concrete, 1st edn. Woodhead Publishing Limited, pp 63–82
13. Greim M (2019) Rheometers for paste, mortar and concrete: measurement technology—possibilities, challenges and limits, in one-day feedback—round robin test: comparison of concrete rheometers: international tests at the Artois University, Paris
14. Macosko C (1994) Rheology, principles, measurements, and applications, Poughkeepsie. Wiley, New Jersey
15. Coussot P (2005) Rheometry of pastes, suspensions, and granular materials. Application in industry and environment. Wiley, New Jersey
16. Ferraris C (1999) Measurement of the rheological properties of cement paste: a new approach, In: International RILEM Conference on the Role of Admixtures in High Performance Concrete
17. Hafid H, Ovarlez G, Toussaint F, Jezequel P, Roussel N (2015) Assessment of potential concrete and mortar rheometry artifacts using magnetic resonance imaging. Cem Concr Res 71:29–35
18. Spangenberg J, Roussel N, Hattel J, Sarmiento E, Zirgulis G, Geiker M (2012) Patterns of gravity induced aggregate migration during casting of fluid concretes. Cem Concr Res 42(12):1571–1578
19. Feys D, Khayat K (2017) Particle migration during concrete rheometry: how bad is it? Mater Struct 50(2):122
20. Zhu H, Martys N, Ferraris C, De Kee D (2010) A numerical study of the flow of Bingham-like fluids in two-dimensional

vane and cylinder rheometers using a smoothed particle hydrodynamics (SPH) based method. J Non-Newton Fluid Mech 165(7–8):362–375
21. Wallevik J (2014) Effect of the hydrodynamic pressure on shaft torque for a 4-blades vane rheometer. Int J Heat Fluid Flow 50:95–102
22. Wallevik J (2008) Minimizing end-effects in the coaxial cylinders viscometer: viscoplastic flow inside the ConTec BML viscometer 3. J Non-Newton Fluid Mech 155(3):116–123
23. Billberg P, Roussel N, Amziane S, Beitzel M, Charitou G, Freund B, Gardner J, Grampeix G, Graubner C, Keller L, Khayat K (2014) Field validation of models for predicting lateral form pressure exerted by SCC. Cem Concr Compos 54:70–79
24. Roussel N, Cussigh F (2008) Distinct-layer casting of SCC: the mechanical consequences of thixotropy. Cem Concr Res 38(5):624–632
25. Perrot A, Rangeard D, Pierre A (2016) Structural built-up of cement-based materials used for 3D-printing extrusion techniques. Mater Struct 49(4):1213–1220
26. Roussel N (2018) Rheological requirements for printable concretes. Cem Concr Res 112:76–85
27. Mechtcherine V, Nerella V, Kasten K (2014) Testing pumpability of concrete using sliding pipe rheometer. Constr Build Mater 53:312–323
28. Kaplan D (2000) Pumping of concrete. PhD dissertation, École des Ponts ParisTech (in French)
29. Feys D, Khayat K, Perez-Schell A, Khatib R (2014) Development of a tribometer to characterize lubrication layer properties of self-consolidating concrete. Cem Concr Compos 54:40–52
30. Kasten K (2010) Gleitrohr-Rheometer—Ein Verfahren zur Bestimmung der Fließeigenschaften von Dickstoffen in Rohrleitungen. PhD dissertation, Technische Universität Dresden (in German)
31. Djelal C, Vanhove Y, Magnin A (2004) Tribological behaviour of self compacting concrete. Cem Concr Res 34(5):821–828
32. Vanhove Y, Djelal C, Magnin A (2004) Prediction of the lateral pressure exerted by self-compacting concrete on formwork. Mag Concr Res 56(1):55–62
33. Roussel N (2006) A thixotropy model for fresh fluid concretes: theory, validation and applications. Cem Concr Res 36(10):1797–1806
34. Amziane S, Perrot A (2017) The plate test carried out on fresh cement-based materials: how and why? Cem Concr Res 93:1–7
35. Zhang M, Ferraris C, Zhu H, Picandet V, Peltz M, Stutzman P, De Kee D (2010) Measurement of yield stress for concentrated suspensions using a plate device. Mater Struct 43(1):47–62
36. Amziane S, Perrot A, Lecompte T (2008) A novel settling and structural build-up measurement method. Meas Sci Technol 19(10):105702